Cartographic and Geometric Components of a Global Sampling Design for Environmental Monitoring

Denis White, A. Jon Kimerling, and W. Scott Overton

ABSTRACT. *A comprehensive environmental monitoring program based on a sound statistical design is necessary to provide estimates of the status of, and changes or trends in, the condition of ecological resources. A sampling design based upon a systematic grid can adequately assess the condition of many types of resources and retain flexibility for addressing new issues as they arise. The randomization of this grid requires that it be regular and retain equal-area cells when projected on the surface of the earth. After review of existing approaches to constructing regular subdivisions of the earth's surface, we propose the development of the sampling grid on the Lambert azimuthal equal-area map projection of the earth's surface to the face of a truncated icosahedron fit to the globe. This geometric model has less deviation in area when subdivided as a spherical tessellation than any of the spherical Platonic solids, and less distortion in shape over the extent of a face when used for a projection surface by the Lambert azimuthal projection. A hexagon face of the truncated icosahedron covers the entire conterminous United States, and can be decomposed into a triangular grid at an appropriate density for sampling. The geometry of the triangular grid provides for varying the density, and points on the grid can be addressed in several ways.*

KEYWORDS: *global sampling design, sampling grid, map projections, polyhedral tessellation, truncated icosahedron, hierarchical grid geometry.*

Introduction

The health of the environment is an issue of global, national, regional, and local concern. Recent trends in energy production and climate change, for example, reemphasize the need for a wide-area focus in assessing the quality of the environment. In this paper we first discuss the salient aspects of a statistically designed environmental monitoring program that is responsive to these concerns. Then we review and analyze several approaches to a global geometry that could be used to implement the statistical design. Finally we describe the properties of a regular sampling grid placed on the surface of an appropriate global model.

Environmental Monitoring to Meet Many Needs

The U.S. Environmental Protection Agency (EPA) is responding to a widely shared view that the United States needs more comprehensive and sound knowledge of the state of the environment by planning a long-term ecological monitoring program (Messer, Linthurst, and Overton 1991). The goal of such a monitoring program is to assess generally the health of the environment across the United States and other parts of North America, and possibly the entire globe. The program will be based upon a comprehensive statistical design in order to obtain sound estimates of the status of, and trends in, the condition of the environment with known degrees of confidence.

Developing the monitoring program requires a design that can sample any spatially distributed and identifiable ecological resource (such as types of forests, lakes and streams, wetlands, estuaries, deserts and grasslands, and agricultural ecosystems) without having an explicit sampling frame available, as there would be in a conventional sampling design for a single resource. The design should lead to explicit probability samples for well-defined populations of resources, but also be flexible, to accommodate the sampling of many different kinds of ecological resources and emerging kinds of environmental stresses.

Specific objectives of the monitoring program for individual ecological resource types are the description of the status, and changes or trends in status, of various biological, chemical, and physical indicators of its health for broad regions of the United States. An important additional objective is determining the association among indicators of sources of environmental stress, exposure to stress, and biological response to stress. This objective prescribes some degree of coincidence in sampling in space and time.

Statistical Design Strategy

The design strategy chosen to meet these objectives is based upon a grid of points at which each ecological resource type will be sampled. The neighborhood of each point will be characterized by ecological and land-use criteria. A collection of sampling units of each resource type in the neigh-

Denis White is a research geographer with METI, U.S. Environmental Protection Agency Environmental Research Laboratory, 200 S.W. 35th Street, Corvallis, OR 97333. A. Jon Kimerling is professor of geography in the Department of Geosciences, Oregon State University, Corvallis, OR 97331. W. Scott Overton is professor of statistics in the Department of Statistics, Oregon State University, Corvallis, OR 97331.

borhood of each point will constitute a Tier 1 sample, to be used to estimate the structural properties of the regional and national populations of these types. The structural properties include the numbers of resource units, their surface area, linear dimension, shape, landscape pattern, and other geometric or geophysical measures obtainable from remotely sensed imagery. A subsample of this Tier 1 sample will be used for field sampling of other attributes of the resources. This double sample (Cochran 1977) will constitute Tier 2 of the design. Field measurements will include, for example, chemical analyses of water samples, visual symptoms of foliage damage to forests, species composition of wetlands, and other indicators of environmental well-being.

The efficient statistical properties of estimates made from the double sample derive in large part from the extensiveness of the Tier 1 sample and the relevance of the information in the data on that sample to the data in the double sample. But a major advantage of this design strategy is that the Tier 1 characterization of areas around the grid points is not restricted to the resources identified a priori. Other resources may be sampled at a later time in response to a new issue regarding their health. The primary design device to implement this adaptive capability is the sampling grid.

Rationale for Cartographic and Geometric Properties of Design

The program objectives and design strategy lead to a set of criteria for the cartographic and geometric properties of the design. The specification of a probability sample requires that the sampling grid be positioned randomly. The most straightforward randomization is by a single random translation of the grid in a plane, followed by the projection of the randomized grid onto the earth's surface. An equal-area map projection is required to preserve the sampling probabilities. The equal-area property also assures that any fixed-size area has the same probability of being sampled, regardless of its location.

Thus, a regular systematic grid of sampling points in the plane of an equal-area map projection best achieves the randomization and equal-area criteria. Additional criteria are that the grid provide compact areas within which to select sampling units, and that it not be aligned with any regularly spaced cultural or physical landscape features. Also, methods for enhancing the density of the grid in a regular hierarchical pattern are useful for increased sampling of rare ecological resources, and methods for reducing the density are useful for implementing regular cyclical sampling in time. Finally, we want a grid system that can conveniently cover the conterminous United States, and be extended to other parts of the country and, potentially, to other parts of the world.

Projecting from the earth's surface to a plane results in area or shape distortion or both. Over large areas of the earth, the magnitudes of these distortions can become quite large. Therefore, it is important to select an appropriately sized and shaped piece of the earth on which to implement the sampling grid. We review below a number of approaches to this problem. Since we have specified an equal-area map projection, the primary concern is with shape (or scale) distortion across the projection surface. However, it is also useful to review and analyze area distortions in otherwise attractive approaches.

Global Framework

Review of Alternative Geometries

A number of approaches to subdividing the surface of the earth in a regular way for large area or global data analysis have been suggested. The approaches can be classified as map-projection approaches, polyhedral tessellations, and adaptive subdivision systems.

Map-Projection Approaches. Existing map-projection coordinate systems provide potential frameworks for subdivision. Tobler and Chen (1986) proposed the Lambert cylindrical equal-area projection as the basis for a quadtree (Samet 1984) referencing and storage system. Their solution attempts to satisfy several principles: regular hierarchical data structuring, easy conversion to other systems, direct relation to latitude and longitude, and equal-area subdivisions. This is achieved by first representing the earth in Lambert's cylindrical projection, then transforming the rectangular representation derived from the cylindrical projection into a square by an area preserving quadrature, and, finally, placing a square grid upon the result. The "vertical" grid lines of this system are meridians spaced at regular intervals and the "horizontal" grid lines are parallels spaced proportional to the sine function. While meeting the authors' requirements, this system has one major disadvantage for our application: the variation in shape of the subdivision cells on the earth, from nearly square at the equator to acute isosceles triangles at the poles.

Mark and Lauzon (1985) proposed an addressing and storage system based upon the Universal Transverse Mercator (UTM) coordinate system. They propose to divide the 60 UTM zones into north to south subzones that are square in the projection plane. (Depending upon the ultimate cell size of the data base, division into east-west subzones might also be necessary.) Each subzone is then further subdivided into a regular square grid of patches, and each patch into a square grid of cells for data storage. Patch and cell addresses can then be implemented as linear quadtree addresses convenient for computer representation. For our use, the UTM-based system has the major disadvantage of not representing the earth's surface in equal-area pieces. It also has major discontinuities in the polar regions, and lesser discontinuities at the edges of the zones.

Polyhedral Tessellations. Another set of approaches to subdividing the world uses knowledge of three-dimensional geometry, first developed in ancient Greece. The Platonic solids are the five regular polyhedra, the tetrahedron, hexahedron (cube), octahedron, dodecahedron, and icosahedron (Coxeter 1948; Pearce and Pearce 1978). These solids can be inscribed in a sphere as the basis of a world subdivision system. Dutton (1989), for example, has proposed using an octahedron as the basis for a system called a quaternary triangular mesh (QTM). The octahedron is

initially aligned with the cardinal points of the latitude and longitude coordinate system; that is, the six vertices are placed at the poles and along the equator at 0, 90, −90, and 180 degrees of longitude. Each triangular face of the octahedron is then recursively subdivided into four subtriangles by placing vertices at the midpoints of the edges, until the size of the faces, or the distance between vertices, is small enough to resolve the features of interest. Dutton calculates that 1-meter resolution is obtained after 21 levels of decomposition. A variation on QTM, proposed by Goodchild and Shiren (1989), uses a different numbering system for the four subtriangles at any level, and provides a straightforward conversion between latitude and longitude and the QTM coordinate system. The QTM systems, like UTM, do not subdivide into equal-area cells, and thus are not suitable for a sampling design specifying the equal-area property.

The dodecahedron has been used by Wickman, Elvers, and Edvarson (1974) for creating a global sampling network. They initially subdivide each pentagon of the dodecahedron into five isosceles spherical triangles, and then recursively subdivide these triangles into four pseudo-triangles. An equal-area subdivision is obtained by connecting edge midpoints with two equal-length great circle arcs joined at a vertex slightly displaced from the single great circle arc connecting the midpoints, so as to create equal areas. The polygons created are four- and six-sided figures, close to triangular in shape. Thus, this system maintains the equal-area property on the sphere. The primary disadvantage for our application is the small irregularities in shape, which prevent the use of a simple randomization scheme.

Fekete (1990) has used the icosahedron as a model for representing data distributions on the sphere. Single-valued spherical surfaces are modeled as triangles whose vertices are projected onto the sphere. The model is initiated with the vertices of the icosahedron, and recursively subdivided as in the QTM models until the error in representing the surface values (not necessarily in resolving location) is below a prescribed minimum. The fourfold recursive subdivision allows an adaptation of the planar quadtree, called the sphere quadtree, for data storage and addressing. As with QTM, the icosahedral tessellation with recursive triangular subdivision does not produce equal-area cells, though the area and shape variation is less than that produced by the octahedral tessellation (see the following analysis).

Adaptive Subdivision Systems. The two preceding approaches are based upon regular decompositions of map projections of the earth to a plane, or upon decompositions of regular polyhedra fit to the earth, or upon a hybrid of these. An alternative approach starts with a given pattern of objects on the earth and tessellates a surface of areal units based upon some property. Lukatela (1987) describes a system for creating the Dirichlet network on a spheroid. The Dirichlet network is also known as the Voronoi or Thiessen network (Upton and Fingleton 1985). This network separates the spheroid into polygons whose loci are all points closest to the set of original points that defined the network. The only sets of points known to result in perfect equal-area Dirichlet tessellations are the centers of the faces of the respective Platonic solids fit to the sphere (Coxeter 1969). Lukatela has described (personal communication), for example, a decomposition starting with the vertices of a dodecahedron and creating the next level of Dirichlet tessellation from the vertices of the preceding level. Only at the level of the original dodecahedron does this approach have regular size and shape cells.

Two previous studies have considered respacing parallels and meridians to obtain equal-area cells on the sphere (or spheroid). Bailey (1956) contrasted the two cases of respacing only the parallels or only the meridians. Paul (1973) investigated several cases of combining both. While obtaining an equal-area subdivision on the sphere, these grid systems do not provide for an equal-area regular grid in the plane, except within a cell. Furthermore, the cells are quadrilateral, and therefore less compact than some other shapes. Another possible adaptive approach not explored in the literature, to our knowledge, is (quadratic) optimization applied to a sphere. Our problem, stated in the language of optimization, is the placement of an arbitrary number of cells on the sphere with an objective function specifying equality of area and compactness of shape. Equality of area could alternatively be specified as a constraint.

A New Approach and Rationale

Based upon our survey of existing proposals for global subdivision systems, we conclude that none meet all of the objectives of equal area, equal and compactly shaped subdivisions with minimal scale distortion, and a hierarchical structure for enhancement and reduction. We also regard existing map projections optimized for coverage of specific areas, such as the standard Albers equal-area conic projection configured for the United States, to be appropriate for those specific areas, but difficult to extend elsewhere. Therefore, we propose a new system based upon an equal-area map projection onto plates of a semiregular (or Archimedean) polyhedron, but with possible adaptations for repositioning the polyhedron to best fit different parts of the earth or for covering large or noncompactly shaped areas of interest. This system uses the truncated icosahedron, a 32-face polyhedron with 20 hexagons and 12 pentagons arranged in a five-way symmetry about a central axis connecting two pentagons. This solid achieves the best compromise among the regular and semiregular polyhedra in meeting the following objectives: faces large enough to cover significant subcontinents (such as central North America, including the conterminous United States); faces small enough to keep scale distortions in map projections to about 2 percent; compact and similar face shapes (hexagon and pentagon); and some degree of familiarity (the pattern often used to construct soccer balls). The systematic sampling grid can then be defined as a regular decomposition of the grid formed by the vertices and center of a hexagon of this model. The map projection we propose is the Lambert azimuthal equal-area projection with a tangent plane. We support our proposal with an analysis of the spherical tessellations of regular polyhedra and, alternatively, map projections upon the faces of these polyhedra. We similarly analyze the truncated icosahedron.

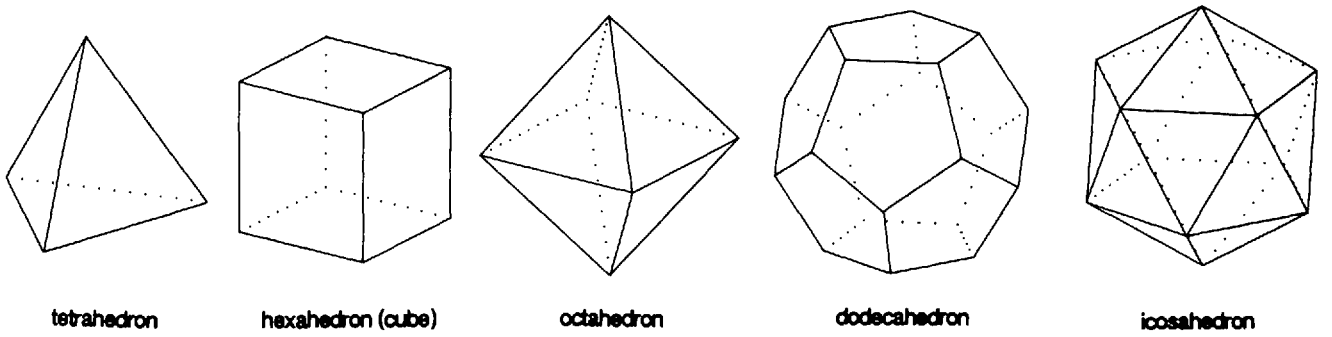

Figure 1. The five regular polyhedra, or Platonic solids.

Table 1. Geometric characteristics of the Platonic solids.

	tetrahedron	hexahedron	octahedron	dodecahedron	icosahedron
face polygon	triangle	square	triangle	pentagon	triangle
number of faces	4	6	8	12	20
number of edges	6	12	12	30	30
number of vertices	4	8	6	20	12
proportion of total area in each face	1/4	1/6	1/8	1/12	1/20

Analysis of Spherical Tessellations of Regular Polyhedra. The five regular, or Platonic, polyhedra are shown in Figure 1 and listed with their properties in Table 1. A circumscribing sphere can be made to touch all vertices of each polyhedron, and polyhedron edges can be thought of as chords of circles that can be projected onto the sphere as great-circle segments, called geodesic lines. These geodesic lines form the edges of spherical triangles, squares, or pentagons that completely cover the sphere and are regular in the sense that all sides and interior angles are equal (Figure 2). The area of each spherical polygon relative to the entire sphere will be the same as in the Platonic solid; for example, each spherical triangle projected from an icosahedron will cover 1/20 of the sphere's surface area. Vertices of spherical polygons with these characteristics are equally spaced, and, hence, provide an ideal set of starting points for subdividing the globe further. Figure 3 portrays one face of each spherical tessellation, using the Lambert azimuthal projection.

Since further subdivision of any of these five spherical polyhedra will produce spherical polygons unequal in size or shape or both, the question of which polyhedron produces the least overall size and shape distortion is of considerable interest. Distortions in size and shape can be studied by subdividing a spherical face of each polyhedron in the same manner, and comparing the areas and interior angles of the smaller polygons formed. It helps if all polygons are of the same degree, which suggests triangulating the faces into a network similar to the triangular networks that comprise geodesic domes (Popko 1968).

The most popular method of triangle subdivision in geodesic construction is called the alternate method (Gasson

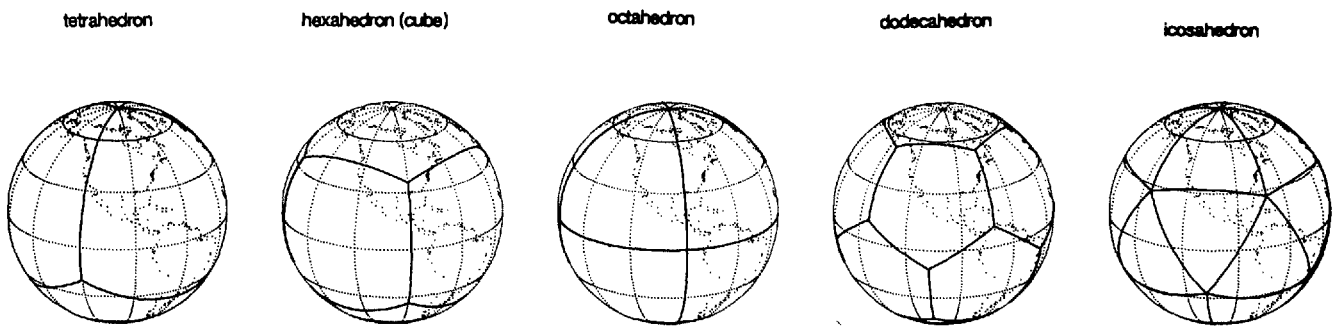

Figure 2. The spherical tessellations of the five regular polyhedra.

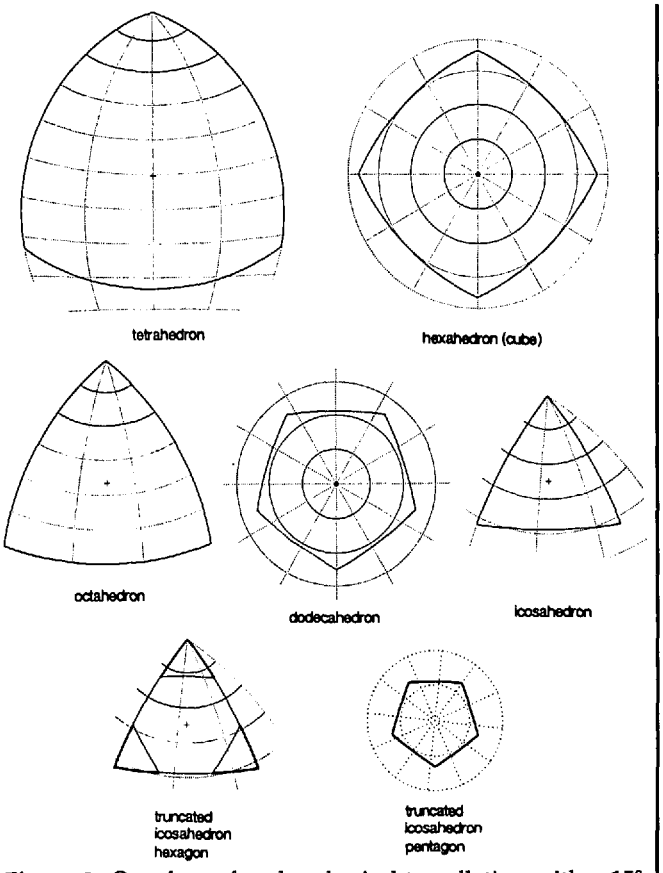

Figure 3. One face of each spherical tessellation with a 15° latitude, 30° longitude, geodetic grid.

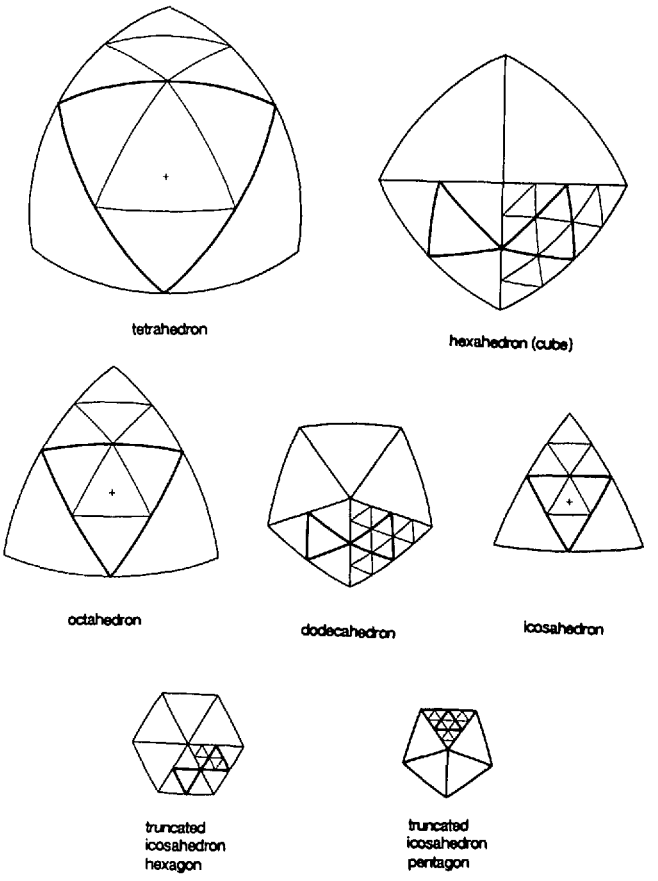

Figure 4. The two- and four-frequency subdivision of one face of each spherical tessellation.

1983), and can be applied directly to the geodesic edge lines for each different spherical triangle. In the alternate method, four new triangles are constructed by creating vertices at the midpoint of each edge of the parent triangle. In the geodesic field, this is called a "two-frequency" subdivision of a triangle. Performing this quartering procedure again produces a "four-frequency" subdivision.

The two- and four-frequency subdivisions of the spherical polyhedra are shown in Figure 4. Cube and dodecahedron faces must be first subdivided into four and five triangles, respectively, that are identical in size and shape, but have only two equal interior angles. Tetrahedron, octahedron, and icosahedron faces are triangular, and the faces for each are identical in size and shape, and have three identical interior angles. The areas and interior angles of these two- and four-frequency triangles on the sphere cannot all be equal, and the deviation in area and interior angles can be determined through spherical trigonometry.

The deviations in spherical triangle areas are given in Table 2 as percentages of the average area for two- and four-frequency subdivisions of each polyhedron. Remembering that the spherical cube and dodecahedron faces have been initially divided into four and five triangles of equal size and shape, respectively, the numbers demonstrate that area differences among triangles generally decrease in proportion to the area of the starting triangle, reaching a difference of zero for infinitely small initial triangles. Average deviations in area also appear to be the same for the two- and four-frequency data, prompting a conjecture that the amount of deviation is independent of subdivision frequency. The range of area deviation is approximately three times the average deviation for all two-frequency subdivisions, and four-frequency subdivisions have a wider deviation range than the two-frequency. Further investigation is needed to determine if the deviation range approaches a maximum limit with increasing subdivision.

The area deviation data point out the benefits of using small initial triangles as the starting point for defining sample points as the vertices of triangles formed by successive quartering. It is also desirable to have sample points from a network of similarly shaped spherical triangles, considering that an initial equilateral triangle network cannot be obtained except from the spherical tessellations of the tetrahedron, octahedron, and icosahedron.

One measure of similarity is the deviation of triangle interior angles from those of an equilateral triangle of the same surface area. This measure can be extended to all triangles in a two- or four-frequency subdivision, giving the average interior angle deviations and deviation ranges listed in Table 2. The icosahedron and dodecahedron subdivisions clearly deviate the least from the equilateral ideal. The average deviation appears to be stable with increasing subdivision frequencies, and the deviation range should slowly increase to a maximum of 30 percent for both. This is primarily due to the starting triangles being small in area and close to equilateral in both cases.

Truncated Icosahedron Tessellation. Subdividing the ico-

Table 2. Deviation in area and interior angles for two- and four-frequency subdivisions of the initial spherical triangles from the Platonic solids.

	tetrahedron		hexahedron		octahedron		dodecahedron		icosahedron	
	2 freq	4 freq	2 freq	4 freq	2 freq	4 freq	2 freq	4 freq	2 freq	4 freq
avg. triangle area (% of sphere)	6.25	1.56	1.04	0.26	3.125	0.78	0.417	0.104	1.25	0.312
avg. deviation (% of avg. Δ area)	50.0	50.0	6.32	6.65	20.19	20.19	2.34	2.34	7.25	7.25
deviation range (% of avg. Δ area)	133.0	226.93	22.17	28.46	53.84	77.54	7.15	9.1	19.33	25.64
avg. interior angle (degrees)	75.0	63.75	62.5	60.625	67.5	61.875	61.0	60.25	63.0	60.75
avg. deviation (% of avg. int. angle)	40.0	40.46	19.12	19.14	18.91	19.4	8.36	8.37	7.34	7.84
deviation range (% of avg. int. angle)	100.0	136.43	66.57	72.86	52.24	69.06	27.11	29.06	21.78	27.9

sahedron and dodecahedron using the alternate method will produce sample points at vertices of spherical triangles that are approximately equal in size and shape, but the maximum deviations are unacceptably large for many sampling systems. Minimizing these deviations requires smaller, hexagonally shaped faces, so that nearly equilateral triangles are formed when the hexagon is triangulated. Such hexagons are a characteristic of the semiregular polyhedron called the truncated icosahedron, one of the 14 Archimedean solids (13 discovered in ancient Greece, the 14th in the 20th century [Lyusternik 1963]). These solids have congruent vertices and regular polygons as faces, but may have more than one kind of regular polygon. The truncated icosahedron (Figure 5) can be conceptualized as an icosahedron, with each of the 12 vertices truncated to form a pentagon, leaving 20 hexagons in the remainder of the 20 original triangular faces. There is only one size of truncation that creates precisely regular pentagons and hexagons from the icosahedron. As with the Platonic polyhedra, a circumscribing sphere can be fit to the 60 truncated icosahedron vertices, and the 90 edges can be projected onto the sphere to form the "soccer ball" pattern, as seen in Figure 5, for the globe.

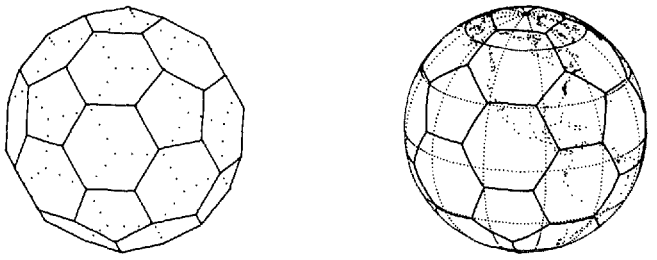

Figure 5. The truncated icosahedron, as polyhedron and as spherical tessellation.

The hexagon of this model is 66.7 percent of the area of an icosahedron triangle, but 71.8 percent of a spherical icosahedral triangle. The total area of the pieces of the three pentagons in one triangle is correspondingly reduced from 33.3 percent to 28.2 percent of the icosahedral triangle. On the globe, the hexagon is large enough to cover the conterminous 48 states of the United States, plus southern Canada and northern Mexico. The truncated icosahedron hexagon is, therefore, an excellent starting point for a large-area triangular sampling grid.

The favorable geometric properties of the hexagonal faces can be seen in Figure 4, which shows a two- and four-frequency subdivision into what appear to be equilateral spherical triangles. This is a slight misperception, since these triangles do deviate slightly in area and shape, as summarized in Table 3. The average deviation of less than 1 percent is a threefold improvement over the dodecahedron subdivision, and the improvement in the deviation range is even better. As with the spherical Platonic solids, the average deviation appears constant with increased subdivision frequencies, and the deviation range increases gradually.

Even more striking is the nearly fivefold decrease in the average deviation in interior angles relative to the icosahedron, coupled with a threefold to fourfold decrease in the deviation range. This translates to angles ranging from approximately 58 to 62 degrees for the four-frequency subdivision. The deviation range increases little with further subdivision, and reaches a maximum of 7.13 percent as the spherical triangles become geometrically indistinguishable from plane triangles. The vertices of these triangles are likely

Table 3. Deviation in area and interior angles for two- and four-frequency subdivisions of the initial spherical triangles from the hexagons and pentagons of the truncated icosahedron.

	hexagon triangles		pentagon triangles	
	2 freq	4 freq	2 freq	4 freq
average triangle area (% of sphere)	0.1496	0.0374	0.1174	0.02935
average deviation (% of avg. Δ area)	0.82	0.82	0.66	0.67
deviation range (% of avg. Δ area)	2.22	2.79	2.20	2.50
average interior angle (degrees)	60.359	60.0898	60.2818	60.07045
average deviation (% of avg. int. angle)	1.56	1.56	11.87	11.87
deviation range (% of avg. int. angle)	6.21	6.91	29.17	29.79

to be the closest to an equal area, equal-shape sampling grid, based on recursively subdividing the sphere across areas the size of the conterminous United States.

A global sampling system based on the truncated icosahedron will have 28.2 percent of the earth's surface falling within the 12 pentagons. Each pentagon can be divided into five identical spherical isosceles triangles (Figure 4), each of which can be further partitioned into two-, four-, and higher-frequency subdivisions, using the alternate method. As seen in Table 3, both the average deviation and the deviation range in the areas of the two- and four-frequency triangles are slightly less than the corresponding triangles from the subdivision of the spherical hexagon. Since each of these five triangles is 78.5 percent of the area of a triangle in the initial division of the spherical hexagon, subdividing in this manner gives triangles 21.5 percent smaller on average than those in the same frequency subdivision of the hexagon triangles.

The average interior angle is also closer to 60 degrees for the pentagon subdivision, but the angular deviation and deviation range is far greater than for the hexagon. This is due to the pentagon triangles not being equilateral, but rather nearly the shape of a 72-54-54 degree plane isosceles triangle. Deviation within the individual angles is small, however, since the maximum range for the larger angle will be from 70.1 to 72.0 degrees, and for the two smaller angles from 54.0 to 55.69 degrees. These values represent the limit of these angles with increasing subdivision.

Map-Projection Surface Tessellation of Polyhedral Faces. A high-frequency subdivision of a truncated icosahedron face produces a triangular sampling grid defined by spherical triangles nearly equal in area and shape. However, this approach suffers in that all triangles differ slightly, and their vertices and distortion characteristics become tedious to compute as the triangular network density is increased to thousands of faces.

A map-projection surface tessellation is another possibility. Here, the polyhedron faces on the sphere are transformed into a planar map-projection surface, upon which a grid of equilateral triangle vertices can be plotted and retransformed into latitude and longitude positions on the sphere or spheroid. The advantages to this approach are several, including the ability to project onto an equal-area map-projection surface so that equilateral triangles on the projection surface define equal-area triangles on the sphere or spheroid. This is accomplished in the map-projection equations, by differentially distorting the map scale along the parallels and meridians so that identical equilateral triangles on the projection surface define triangles of equal area, but continuously varying shape, on the globe. The advantage over directly subdividing the sphere is that the shape distortion is gradual, and can be computed easily for every sample point, as can the geographic coordinates.

Equal-area map projections of Platonic solids and truncated icosahedron faces are illustrated in Figure 6. The Lambert azimuthal equal-area map projection was used throughout because shape distortion is the same along any circle of a given radius from the projection center. If the polyhedral face center is made the projection center, shape distortion will vary in a circular pattern away from the center, and a projection surface with a minimal range in shape distortion will result, due to the symmetry in each polyhedron face. This projection produces the shape distortion

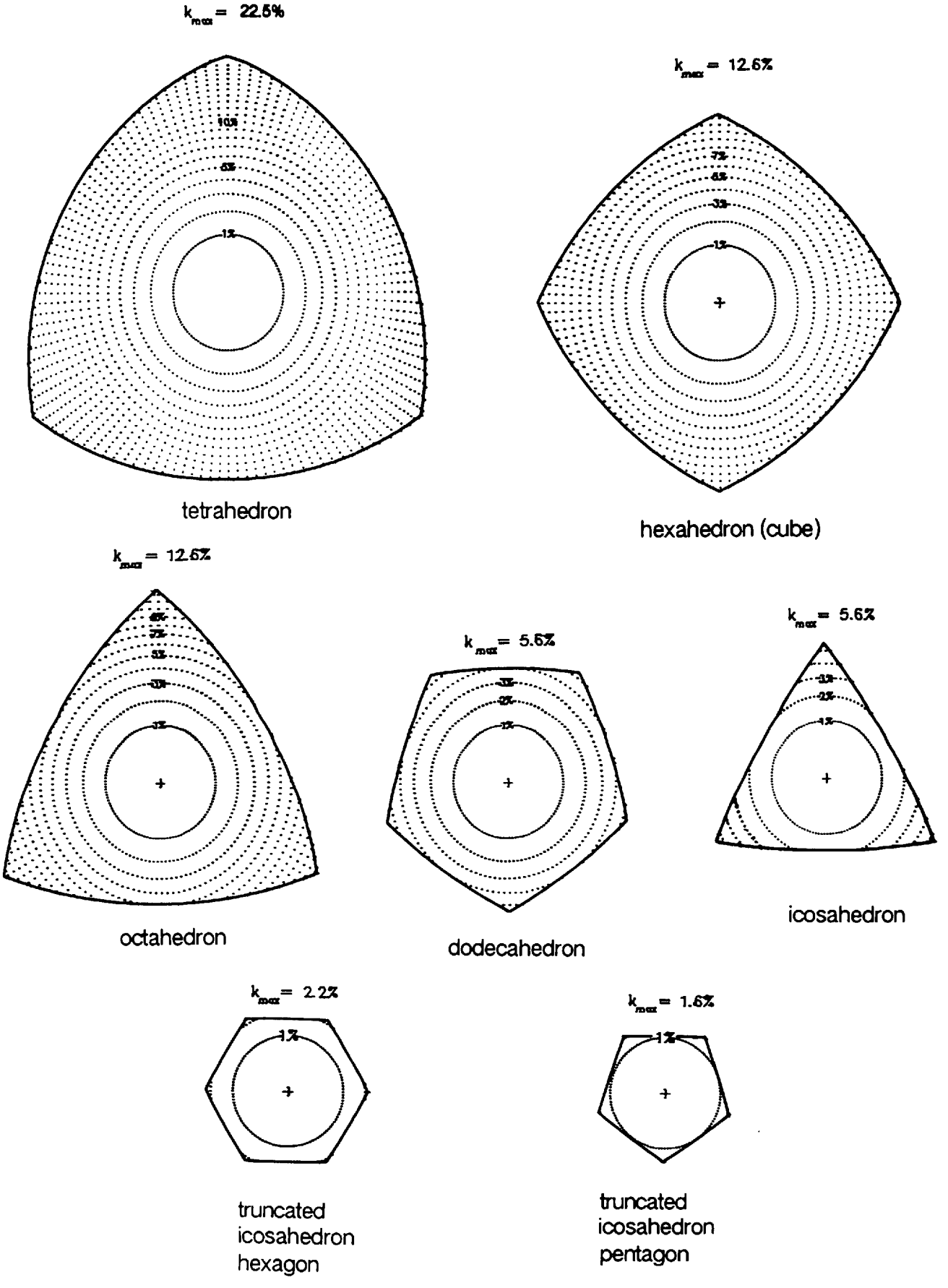

Figure 6. The 1-percent scale distortion contours from the Lambert azimuthal equal-area projection of one face of each spherical tessellation.

indicated by the concentric circles in Figure 6. These circles are the contours of distortion along the parallel (k distortion) in 1 percent increments.

These distortion maps show the expected decreases in shape distortion with decreasing face sizes. The map-projection surface for the tetrahedron spherical face has the greatest distortion, with the map scale along the parallel at the farthest face edge being more than 22 percent larger than the scale at the face center. In an equal-area projection, the map scale along a meridian (h distortion) at a face edge must then be 18-plus percent smaller ($h = 1/k = 1/1.225$) than at the zero-distortion face center. The maximum shape distortion is less on the projected faces of the cube and octahedron, and still less on the projections of the dodecahedron and icosahedron faces. Because of its small size and roughly circular shape, the truncated icosahedron hexagon face has the lowest maximum distortion of all these figures. Here, the map scale at the farthest face edge is a maximum of 2.2 percent larger along the parallel, and 2.2 percent smaller along the meridian. The conterminous United States easily falls within the 2 percent scale distortion circle.

The difference between determining sample points by recursive subdivision of spherical polyhedra faces, and by subdivision of equilateral triangles on an equal-area map projection of the spherical faces can now be stated more clearly. Direct subdivision of the spherical face produces a network of sample points that is nearly regular in the area and shape of the triangles that define the point locations. The triangles are, however, slightly different in area and shape, with some being close to the equilateral ideal, and others deviating significantly. The triangles defined on the Lambert projection, on the other hand, are equal in area and represent equal-area spherical triangles on the globe. The shape distortion introduced by the Lambert equal-area map projection is systematic, easy to compute, and smaller in range than the distortion introduced by recursive subdivision directly on the sphere.

A similar subdivision procedure will create a grid of ever smaller 72-54-54 degree isosceles triangles on each pentagon face. These will be 20.5 percent smaller in area than hexagon triangles for the same subdivision frequency. Figure 6 shows a maximum scale distortion at each edge vertex of 1.6 percent along the parallel. The 0.6 percent difference in maximum scale distortion on the pentagon and hexagon faces is due to the polyhedron being slightly modified to circumscribe the globe. This means that the center of each hexagon and pentagon touches the globe, but the distance between the globe center and hexagon edge vertex on the projection surface is 2.65 percent longer than for the same vertex on the adjacent pentagon projection surface. The formulas for the Lambert projection transform this difference in distance to 0.6 percent, meaning that the (x, y) projection coordinates for each pentagon must be multiplied by a 1.006 scaling constant if the distance between two edge vertices on the projection is to match the distance between the same two vertices on the hexagon projection. This small-scale enlargement required for creation of perfectly matching polyhedron vertices must be taken into account when computing the areas of triangles on the pentagon face.

Interfaces Between Adjacent Faces, and Pentagon Grids

The Lambert azimuthal map projection transforms vertices of a spherical hexagon and pentagon into vertices of regular hexagons and pentagons on the projection plane. The geodesic lines between vertices that bound each spherical polygon are not projected as straight lines, but rather as slight curves bowing outward from the projection center. This complicates the generation of sample points on the projection surface, since regular hexagons and pentagons on the plane are required for points to be vertices of triangles of equal area and shape. These can be created only by equally spacing a row of sample points along each edge of a planar regular hexagon or pentagon, according to the desired sampling density.

This procedure introduces the problem of how to set sample points within the "slivers" created between the planar polygon edges and the slightly bowed spherical polygon edges. These slivers are narrow (36.2 km and 28.5 km maximum widths for the hexagon and pentagon edges, respectively), meaning that "lune-like" slivers with maximum widths of 72.4 and 64.7 km, respectively, are formed between hexagon-hexagon and hexagon-pentagon edges.

One solution is to place additional points in the sliver between two adjacent sampling grids. One method for this is to extend the triangular grid from one of the two adjacent hexagons into the sliver, clipping to the sliver boundary. Figure 7a is a schematic illustration of how the sliver (greatly exaggerated in width) appears in the Lambert projection with two hexagons meeting in a straight line, and the great circle dividing the sliver projected as an arc into the op-

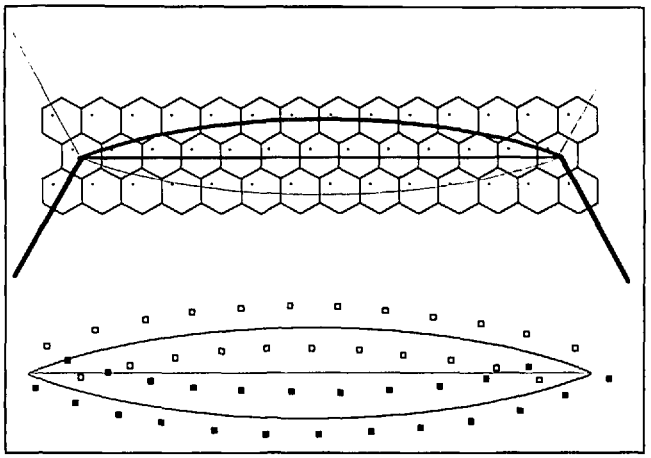

Figure 7. Spherical slivers between plane hexagons in the Lambert azimuthal and gnomonic projections (exaggerated in width for illustration purposes). (a) Top: A randomized grid across two adjacent hexagons, each shown in the Lambert azimuthal projection. Each hexagon's portion of the sliver is shown as a half-lune from the straight hex edge to the great circle arc separating the hexagons. The great-circle arc between the hexagons thus appears twice. (b) Bottom: A randomized grid across two adjacent hexagons in the gnomonic projection. The great-circle arc between the hexagons is shown in a thin line. Sample points from each hexagon are extended by one row into the sliver.

posite hexagon. Figure 7b illustrates the situation in a gnomonic projection, which represents the great circle between two hexagon vertices as a straight line and the hexagon edges as arcs. The interface between a hexagon and a pentagon can be handled in a similar way.

A more elegant solution is to "unbow" each edge of the projected spherical polygon by modifying the map-projection equations to produce regular hexagons and pentagons. John Snyder (1991) has very recently devised such a projection, to be called the Equal-Area Polyhedral Projection. After deriving this projection, he found that Irving Fisher had used the same concept in a design for the icosahedron, reported as a footnote in Bradley (1946), but Snyder has carried the derivation further, to include other polyhedra, inverse formulas, and distortion analysis. Snyder's idea is best understood by examining one of the six equilateral triangles forming a pole-centered hexagon (Figure 8). The scale in the meridional direction has been progressively reduced from the edge to the center of the triangle base. This reduction allows the geographic coordinates of positions along the great-circle triangle base to be projected to a straight line, eliminating the slivers between adjacent faces. The projection is made equal area by adjusting the spacing of meridians from the edge to center of the triangle, resulting in a maximum angular deformation of 3.75 degrees and a maximum scale distortion of 3.3 percent. Since this is done for the six hexagon edges, all hexagon-to-hexagon edges will match exactly. The Equal-Area Polyhedral Projection can also be applied to the five isosceles triangles composing each pentagon. Pentagon-hexagon edges match to within 1 part in 10^5 of the length of a side.

The placement of a grid on a pentagon of a truncated icosahedron introduces additional issues. An equilateral triangular grid cannot include the vertices of a pentagon. One solution is to divide the equal-area projected surface of the pentagon into five isosceles triangles, and subdivide these into congruent triangles such that the spacing between points and areas of the triangles are close to those of the equilateral triangles of the hexagon grid (Figure 9a). A second possibility is to extend the five adjacent hexagon grids into the adjoining triangle of the pentagon, or, in effect, to use the icosahedron as the model solid (Figures 9b and 9c). As shown above, this sacrifices the low distortion characteristics that can be achieved on the projected hexagons and pentagons of the truncated icosahedron.

Advantages and Disadvantages of Different Global Configurations

For the application of this global tessellation to a sampling network for the conterminous United States, we have positioned the solid such that one hexagon covers all of the land area in the conterminous states and nearby coastal waters, and such that a neighboring hexagon covers all of Alaska, except the end of the Aleutian chain of islands (Figure 10). Also note that the Hawaiian Islands fall within a third hexagon. In placing the truncated icosahedron to optimize the coverage of central North America with a single hexagon, other parts of the world may naturally be less

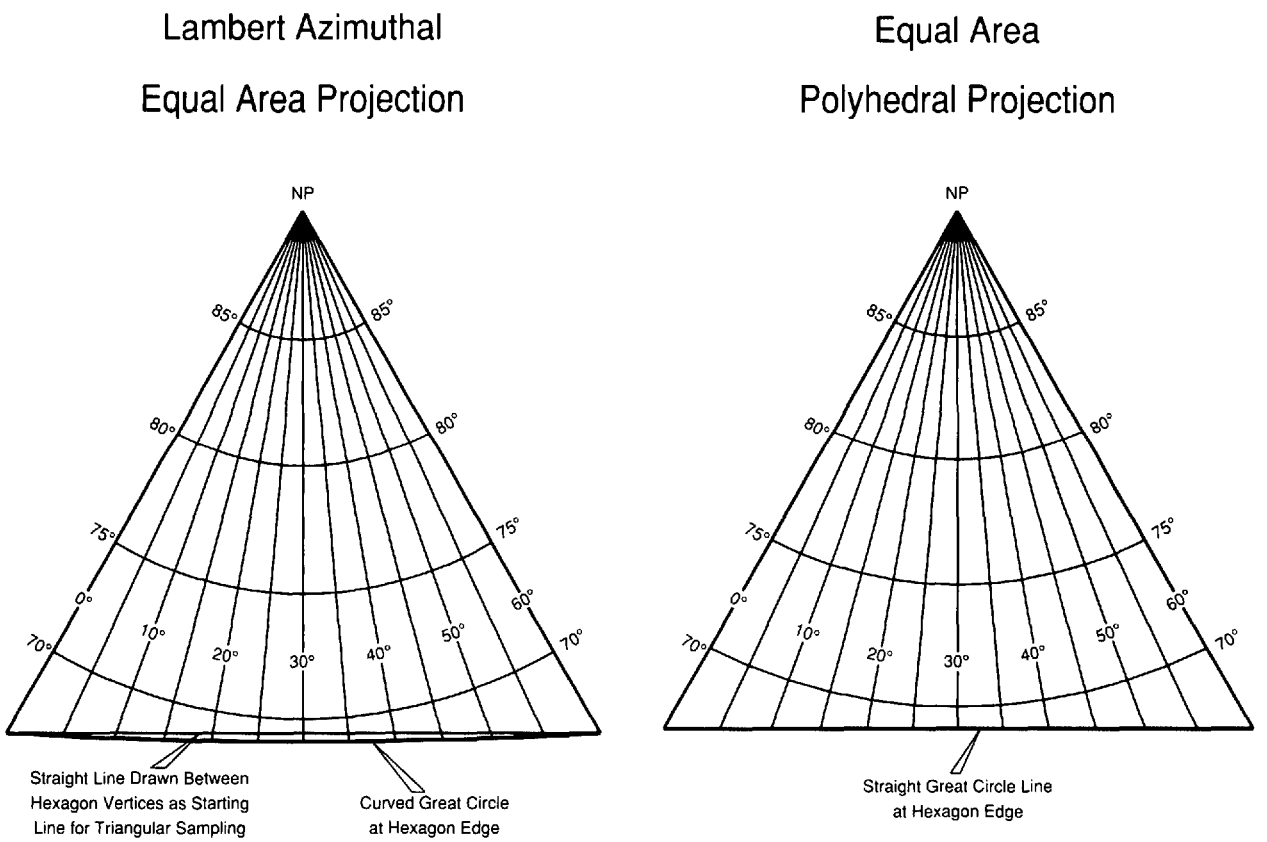

Figure 8. The Lambert Azimuthal Equal-Area and the Equal-Area Polyhedral (designed by John Snyder) map projections of one-sixth of a truncated icosahedron hexagon, centered on the North Pole.

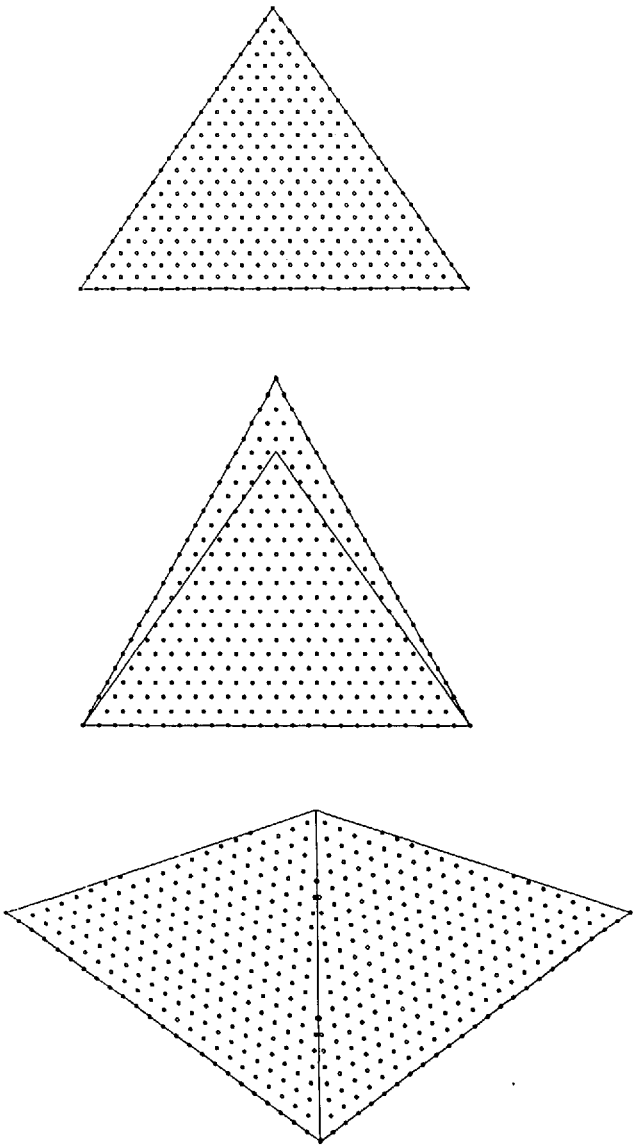

Figure 9. Placement of regular grids on the pentagon of the truncated icosahedron. (a) Top: Sample grid placed on one of the isosceles triangles. (b) Middle: The hexagon grid (larger triangle) clipped to the pentagon triangle. (c) Bottom: How the hexagon grid meets on two adjacent pentagon triangles.

well covered. Several alternatives are possible for addressing the placement of sampling grids in different parts of the world. One, of course, is to use this particular configuration as it extends across the globe. Second, a less-specific configuration could be used. Third, no single configuration need be specified; rather, an adaptive solution suited to any area of interest could be used.

Several criteria are not important in choosing one of these alternatives. For making global or continental scale estimates of population attributes, the lack of coherence among different geometries from different sampling designs is not a problem, as long as the probability structures of the various designs are known. Mapping discrete or continuous population distributions for the globe, or for large areas of the globe, also is not affected by different sampling geometries, as long as the conversion to some standard coordinate system is known. And the incorporation of data from different sampling designs into global or continental scale ecological or geophysical models is likewise not limited by different sampling geometries, since data can be placed into a common georeferencing system, either as aggregate population estimates or as individual sampling observations whose location coordinates are converted to a common system.

Extending the configuration for good coverage of central North America, Alaska, and Hawaii takes advantage of the existing cartographic development and provides good coverage for several other parts of the world, most notably the Indian subcontinent and central South America. Unfortunately it splits Europe into east and west, and divides Japan into two hexagons. This configuration is shown in three orthographic views in Figure 11.

An alternative fixed configuration of the truncated icosahedron can be labeled the polar configuration, as it is the natural orientation for a rotational sphere. In this case, the centers of two pentagons are placed at the poles, and the pattern is fixed about the rotational axis of the earth by arbitrarily locating one of the meridional edges between two hexagons along the Greenwich meridian. This configuration avoids any element of chauvinism, and perhaps best relates to other standard reference systems such as latitude-longitude. Study areas such as the north polar region are covered symmetrically with this placement; however, many other areas require several faces, including many that could be covered well by a single hexagon, such as Australia and Europe. This configuration is shown in the Hammer-Aitoff projection in Figure 12.

The final alternative is to recognize again that there is no known optimal tessellation figure, and no optimal configuration pattern for the truncated icosahedron as a compromise model. Since the primary objective of this geometric model of the earth is for probability sampling, and since we specify an equal-area map-projection approach as best suited for this objective, an adaptive policy toward global configurations has certain advantages. In this view, each area of interest on the earth is covered by the best configuration of truncated icosahedron faces, or possibly by other models and associated projections. In many, if not most, cases, the truncated icosahedron faces with the Lambert azimuthal projection provide a good compromise between area of coverage and map-projection distortion. Such an adaptive approach requires mechanisms for reconciling overlapping grids from designs developed on different centers, or for creating seams between such designs. This problem is similar to the seam problem between adjacent hexagons, and between hexagons and adjacent pentagons on the truncated icosahedron.

Implementing a Sampling Grid in the Plane of a Truncated Icosahedron Hexagon

Systematic Point Grids in the Plane

The three regular polygon tessellations in the plane (Coxeter 1969), the triangular, square, and hexagonal tessellations, have corresponding dual-point grids—the hexagonal, square, and triangular grids—whose points are the centers

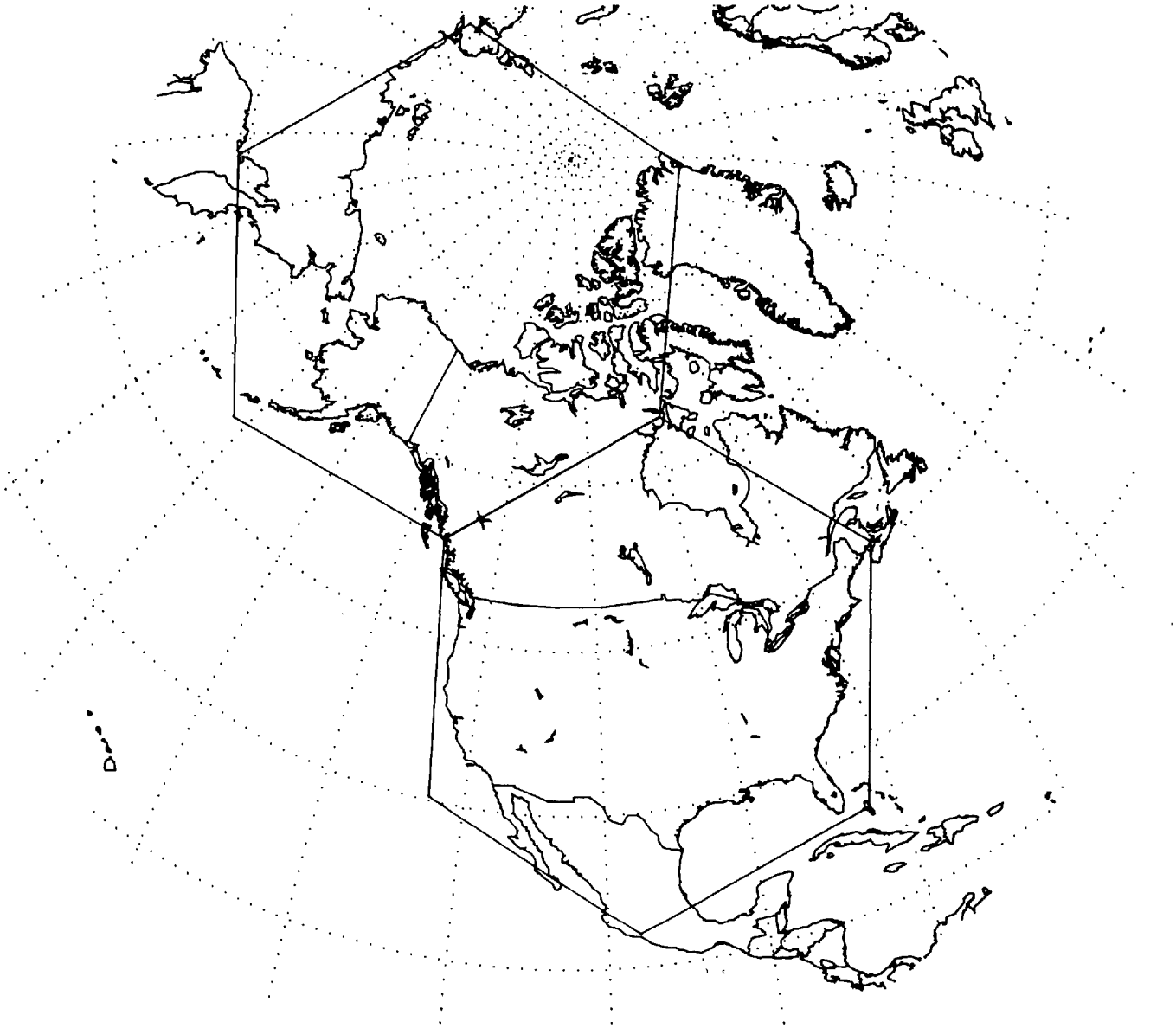

Figure 10. Hexagons of the truncated icosahedron covering central North America and Alaska.

of the corresponding polygons (Figure 13). Any of the three can define an equal-area sampling network. The triangular grid and its corresponding hexagonal tessellation have the advantage of being the most compact and isotropic. Furthermore, some modest statistical advantages accrue to the triangular grid because of its geometric properties (Switzer 1975; Olea 1984; Matérn 1986). The square grid has the advantage of most frequent and easy application. The triangular tessellation and its corresponding hexagonal point grid appear to have little advantage for our application. We choose to use the triangular grid to take advantage of compactness and greater directional freedom.

Hierarchical Decomposition of Triangular Grids

The triangular grid can be decomposed in several ways. The theory for these decompositions is contained in the algebraic theory of groups (Dacey 1964; Hudson 1967). The three lowest-order decompositions (aside from the identity decomposition) that maintain the triangular structure, and hence uniform probabilities under randomization, result in increases in density by factors of 3, 4, and 7. (The literature of central place theory in economic geography describes these hierarchies as applied to the dual tessellations of hexagons [Christaller 1966; Lösch 1954]).

To implement these decompositions, we can develop algorithms for transforming a grid to a higher density. In order to provide a consistent description, each algorithm for density enhancement is described as a transformation in the plane of a unit figure containing the additional points. The algorithms are applied to the unit figure associated with each original grid point. For this presentation, the original grid is assumed to be aligned such that one of its three axes is parallel to the x axis of the cartesian grid.

For the threefold enhancement, the unit figure is an equilateral triangle with one vertex, corresponding to a point

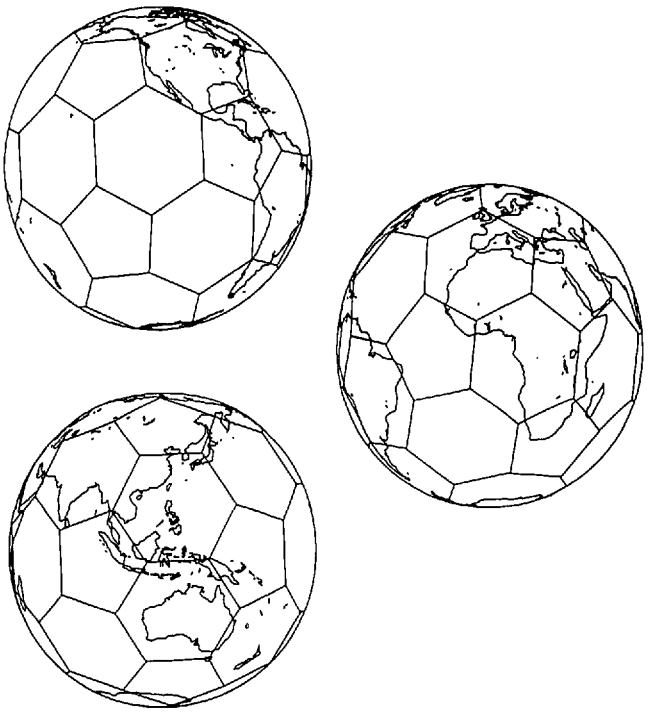

Figure 11. The truncated icosahedron as placed on the globe for optimal coverage of the conterminous United States, Alaska, and Hawaii shown in three orthographic projections.

on the original grid, at the origin, a second point at $(-1/2, -\sqrt{3}/2)$, and the third at $(1/2, -\sqrt{3}/2)$. The second and third points of the unit figure are scaled by $d/\sqrt{3}$, where d is the distance between points in the original grid, and rotated by $\pi/6$ (Figure 14). Since there is three-way symmetry in a triangular grid, two threefold enhancements bring the grid back into the original alignment. An alternative way to conceptualize this is by placing an additional point at the geometric center of each triangle formed by three neighboring points in the original grid (as, for example, in Mandelbrot [1988]).

For the fourfold enhancement, the unit figure is a rhombus with one vertex, corresponding to a point on the original grid, at the origin, a second point at $(-1/2, -\sqrt{3}/2)$, a third at $(1/2, -\sqrt{3}/2)$, and the fourth at (1,0). The last three points are scaled by d/2, d defined as above. There is no rotation in the fourfold enhancement (Figure 15). An alternative way to conceptualize this is by placing an additional point halfway between all pairs of neighboring points in the original grid.

For the sevenfold enhancement, the unit figure is a hexagon whose center is a point on the original grid and whose vertices are (0,1), $(-\sqrt{3}/2,1/2)$, $(-\sqrt{3}/2,-1/2)$, $(0,-1)$, $(\sqrt{3}/2,-1/2)$, $(\sqrt{3}/2,1/2)$. The six points of the hexagon are scaled by d/7, d defined as above, and rotated by -arctan $(1/3\sqrt{3})$ (Figure 16). (See Richardson [1961] and van Roessel [1988] for related discussions.) Alternating sevenfold enhancements can realign with the original grid by alternating the sign of the angle of rotation.

The geometric logic of enhancement applies as well to reductions of an original grid, with the algorithms appropriately inverted. Furthermore, these basic factors of enhancement and reduction may be combined to achieve many additional factors. Thus, a sevenfold enhancement with a fourfold reduction results in a 7/4 increase in density. In our application, the enhancements will typically be used to increase the density of sampling for rare resources, and the reductions for periodic cycles of sampling in time.

Base Grids for Sampling

A hexagon is a convenient figure from which to create a triangular grid, since the vertices and the center form a seven-point starting grid. A suitable compromise between

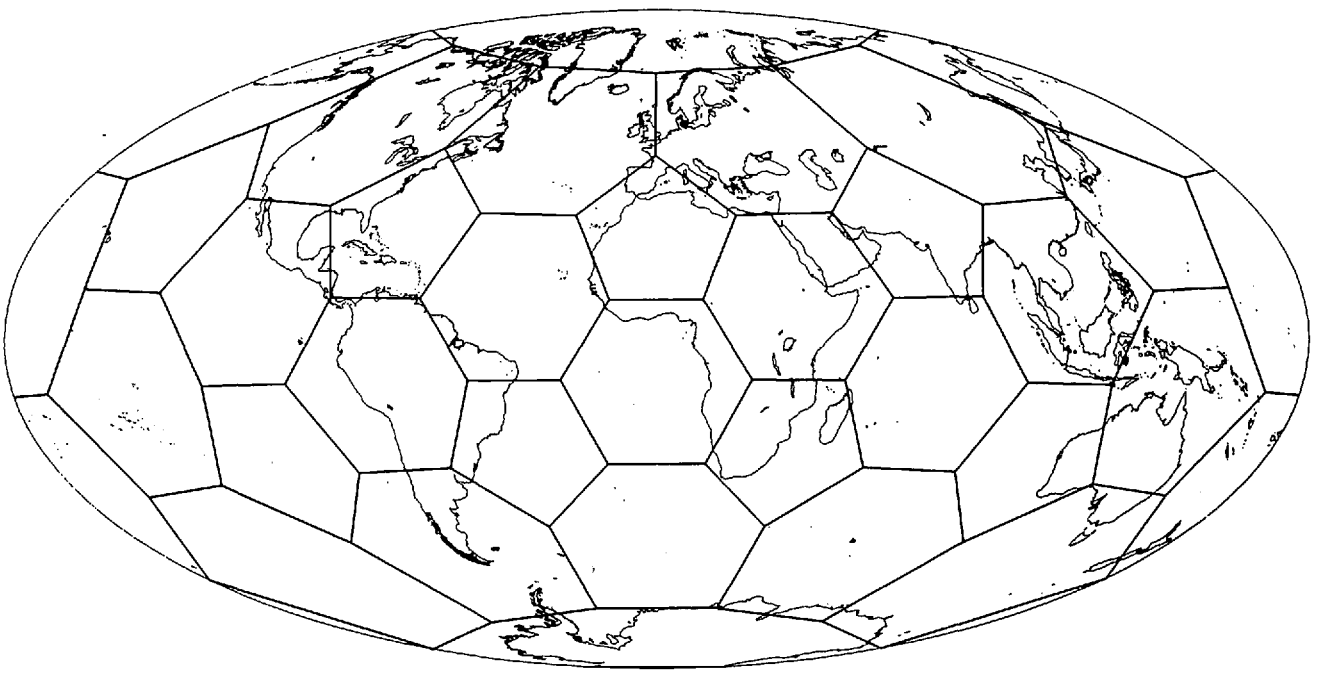

Figure 12. The polar configuration of the truncated icosahedron shown in the Hammer-Aitoff projection.

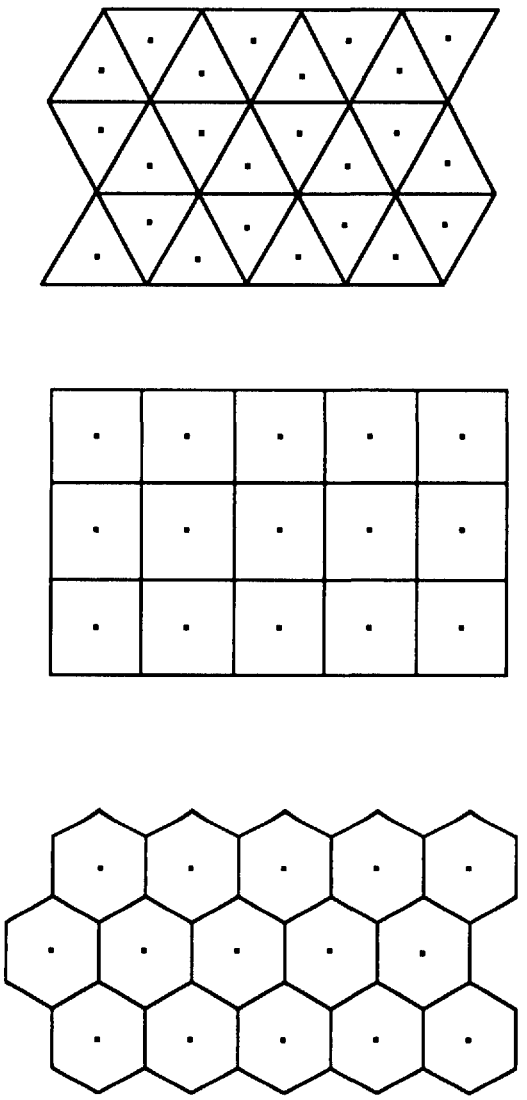

Figure 13. Regular tessellations in the plane with corresponding dual-point grids. (a) Top: Triangular tessellation with hexagonal grid. (b) Middle: Square tessellation with square grid. (c) Bottom: Hexagonal tessellation with triangular grid.

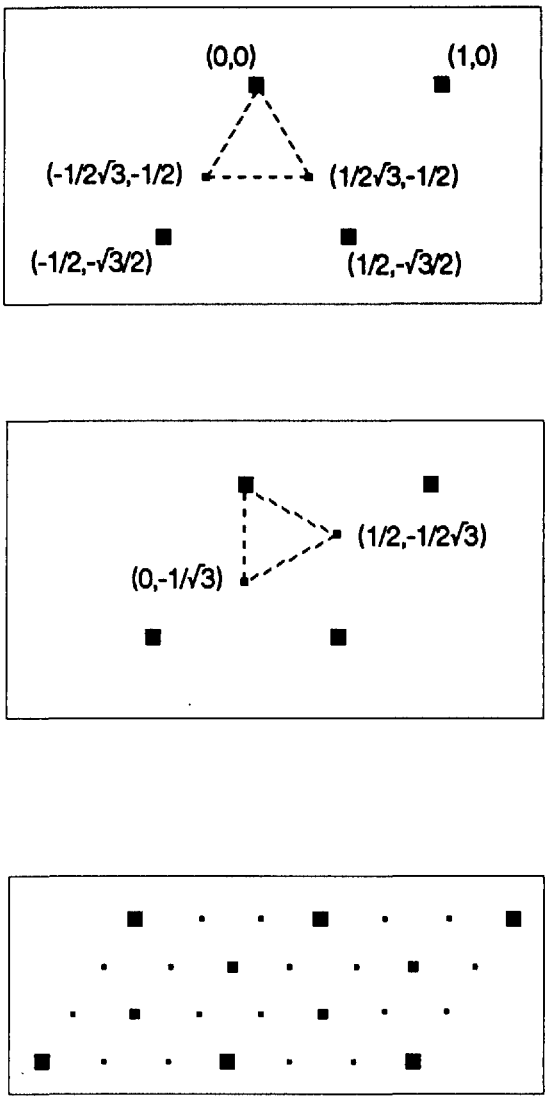

Figure 14. Threefold enhancement and reduction. (a) Top: Unit figure scaled to unit grid; before rotation. (b) Middle: After rotation by $\pi/6$; enhancement complete. (c) Bottom: Three levels of the threefold decomposition hierarchy.

the desired spatial resolution of sampling and the projected available financial resources can determine the density of a base sampling grid. For our application, an approximately 640 square km hexagon tessellation about the points, corresponding to a distance between sampling points of approximately 27 kilometers, has been suggested. This can be very closely realized with a decomposition of the hexagon of the truncated icosahedron by a factor of $3^2 * 4^5$, or two enhancements by 3 followed by five enhancements by 4. The increase in density is by a factor of 9,216, corresponding to a linear increase by a factor of 96. Thus, each edge of the large hexagon can be divided into 96 equal parts and the derived points connected to obtain a triangular grid for this base sampling density containing 27,937 points.

Addressing Systems

Uniquely identifying points on the sampling grid is necessary for assigning attributes to the points. The simplest system is to number sequentially by rows and to number within rows of one of the axes of the grid. Enhancements in grid density require additional numbers, or addresses, in the sequence, and a history of awarded numbers to avoid duplication. Two other addressing systems merit attention.

The first is a cross-reference system with existing coordinate systems. The most useful of these is the standard geographic system of latitude and longitude. Each point can be assigned a pair of numbers in latitude and longitude (or a concatenated or interleaved single number) with sufficient precision to uniquely specify the point. In particular, since the maximum distance that occurs in a 7.5-minute quadrangle in the conterminous United States is less than 20 kms, and hence there can be no more than one base sampling point in any quad, the numbering convention adopted by the U.S. Geological Survey for these large scale topographic quadrangles could be effectively used (USGS 1985). The potential for enhancement of density also complicates this approach, requiring enough digits of precision

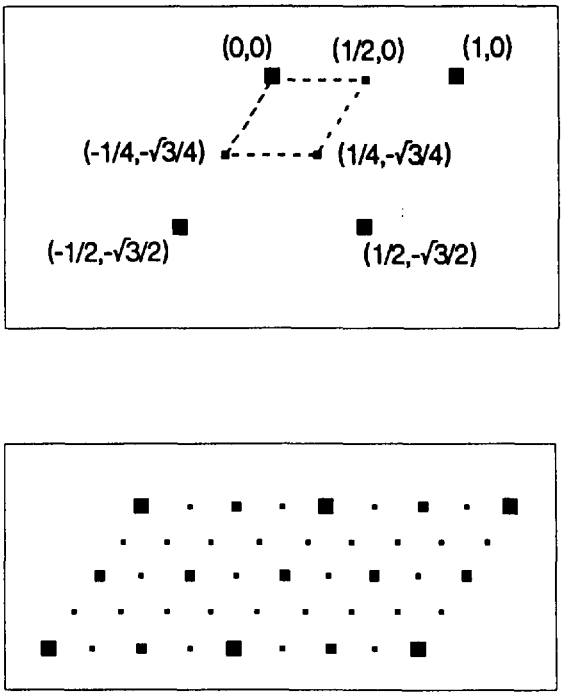

Figure 15. Fourfold enhancement and reduction. (a) Top: Unit figure scaled to unit grid; no rotation needed, enhancement complete. (b) Bottom: Three levels of the fourfold decomposition hierarchy.

to be reserved in advance, or the use of additional identification for enhanced grid points.

The second system makes use of the decomposition geometry to construct a single hierarchical identification system. This approach is analogous to that of Dutton (1989), Goodchild and Shiren (1989), and Wickman and others (1974) for their respective polyhedral systems; it is also analogous to that of Morton (1966) and Gargantini (1982) for square hierarchies in the plane and Gibson and Lucas (1982) for hexagonal hierarchies in the plane (and higher dimensions). In our system of mixed hierarchies (Lindgren 1967; Woldenberg 1982), both a radix or base number and a digit in that radix need to be specified. In Figure 17, the digit conventions are given for the threefold, fourfold, and sevenfold systems, respectively. At any finer level of the threefold, fourfold, or sevenfold hierarchy, a ternary, quaternary, or septenary digit, respectively, uniquely identifies the points derived from a single point on the coarser level. A two-digit address (without radix) is shown for a point in a two-level, fourfold hierarchy in Figure 18a.

When mixing hierarchies, the composition of enhancements is commutative, so that there is more than one address for a point, but no two points can have the same address. One possible notation for addresses in the mixed environment is left-to-right concatenation of successive levels of decomposition with subscripts indicating the radices. An example with a two-level, fourfold-by-threefold hierarchy is shown in Figure 18b.

Since the base grid is fixed in our application, a condensation of addresses for these points may be achieved by combining the two threefold enhancements into a nonanary (radix 9) digit, followed by five quaternary digits for the five fourfold enhancements. With positional order as-

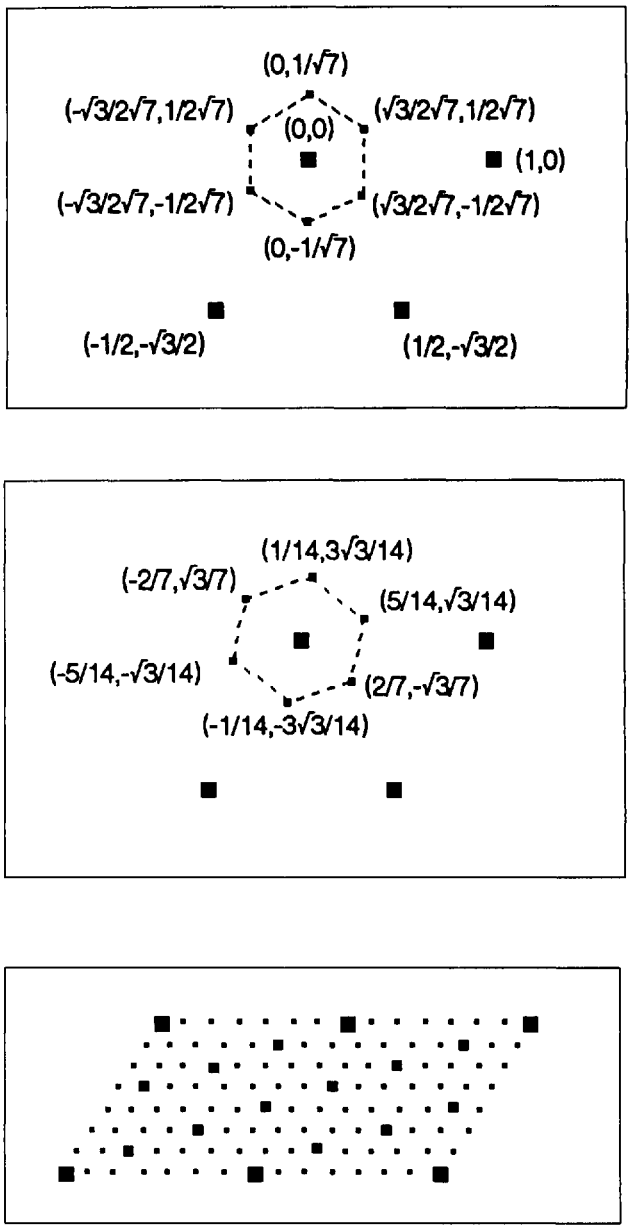

Figure 16. Sevenfold enhancement and reduction. (a) Top: Unit figure scaled to unit grid; before rotation. (b) Middle: After rotation by $-\tan^{-1}(1/3\sqrt{3})$; enhancement complete. (c) Bottom: Three levels of the sevenfold decomposition hierarchy.

signed and thus no radix digits required, only a six-digit address for the baseline points is necessary for the decomposition from one of the four rhombuses, or part rhombuses (triangles), of the North American hexagon. Adding a digit on the front of the address for the initial rhombus makes a total of seven. This scheme is shown in Figure 19. The four rhombuses, or parts, are numbered as in the fourfold enhancement system. Therefore, for example, the rhombus beneath (to the south of) the center of the hexagon, extending to but not including the grid rows joining the three large hexagon vertices southeast, south, and southwest of the center, is number 3. It is subdivided into nine rhombuses numbered 0 to 8 northwest to southeast within row, and northeast to southwest across rows. This

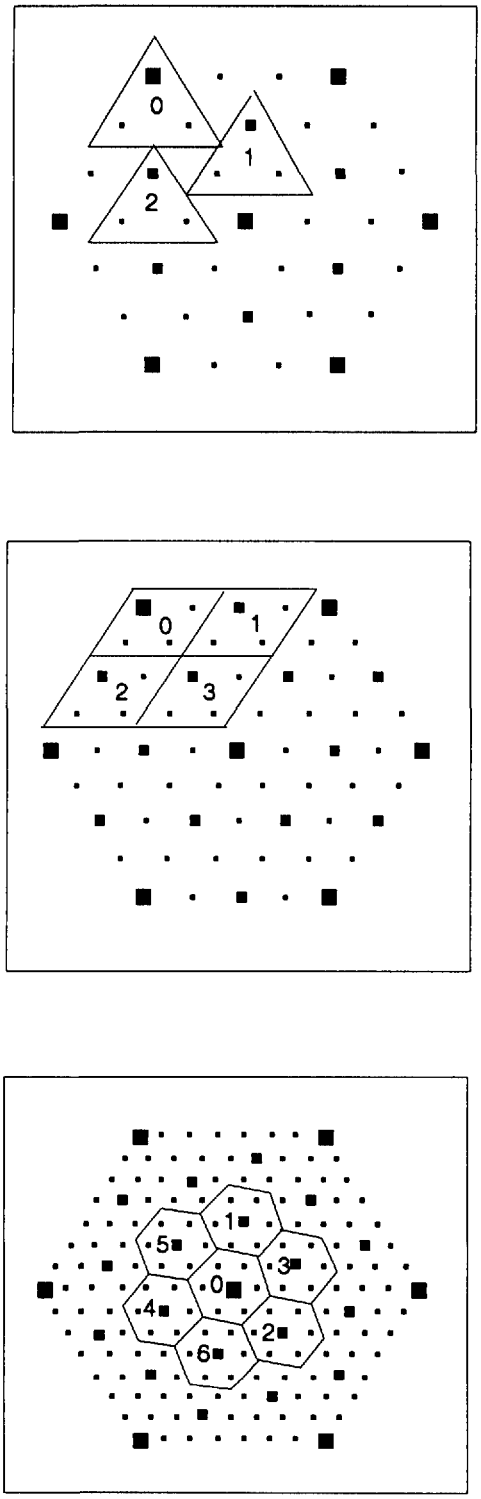

Figure 17. The three addressing systems. (a) Top: Threefold system. (b) Middle: Fourfold system. (c) Bottom: Sevenfold system.

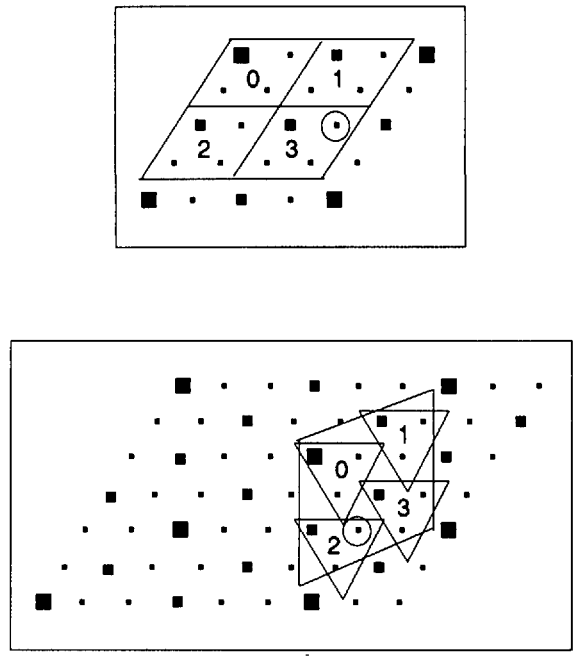

Figure 18. Addressing examples. (a) Top: The address of the circled point is 31 in the two-level, fourfold system. (b) Bottom: The address of the circled point is $2_4 1_3$ in the two-level, fourfold-by-threefold system.

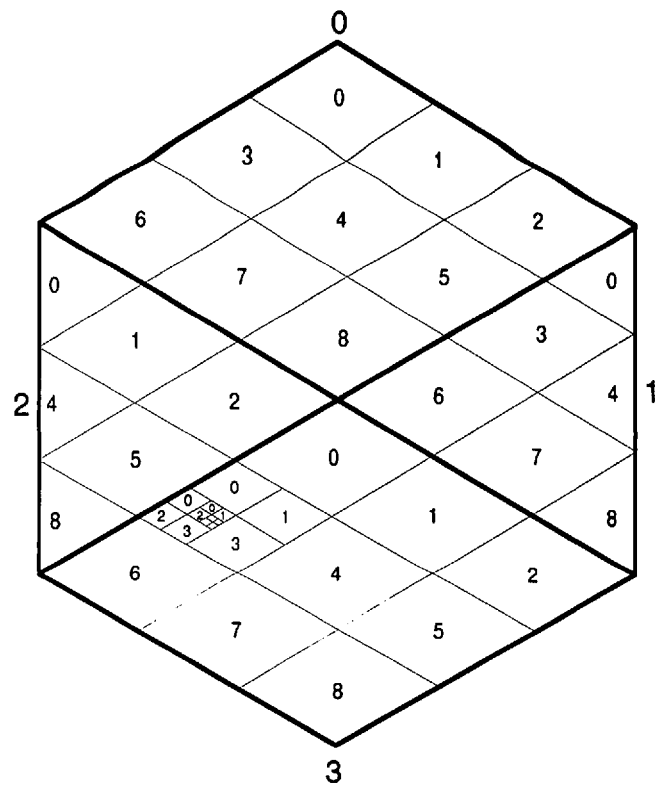

Figure 19. Baseline addressing scheme for a hexagon from the truncated icosahedron. The five highest-order digits are shown in one area.

accounts for the two threefold enhancements in the baseline grid. Rhombuses are then successively quartered five times to identify a single point. An example address on the grid of the North American hexagon is shown in Figure 20. Alternatively, four of the five fourfold enhancements could be represented by two hexadecimal digits, with a single quaternary digit at the end, further condensing the address. This addressing system could form the basis for a modified quadtree storage system, where the second level has nonanary rather than quaternary nodes, requiring modifications to quadtree access and searching algorithms.

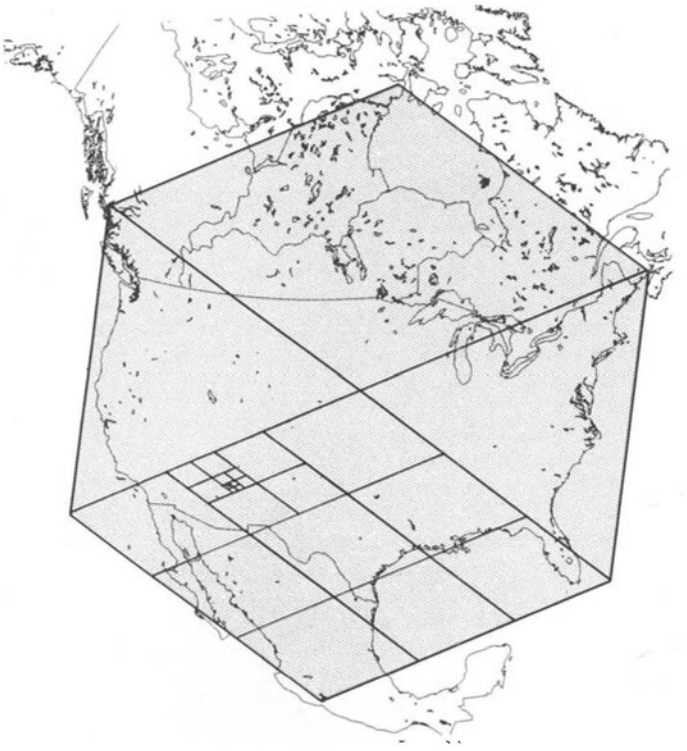

Figure 20. Baseline sampling grid with addressing for the North American hexagon. The darkened point's address is 3321320, or 339E0 using hexadecimal condensation.

For identifying sample points uniquely across adjacent faces of the truncated icosahedron model, an additional level of addressing would be necessary to specify the face. Points introduced in the seam between two faces also would need special treatment. For points derived from a different global configuration of the truncated icosahedron, identification of the configuration also would be necessary.

Summary

We have described the cartography and geometry of a sampling design that can address a wide variety of environmental issues, especially the assessment of the environmental quality of major ecological resources. This design is fundamentally based upon a systematic grid of sampling locations placed on the plane of an equal-area map projection from the surface of the earth. The plane can be construed as the face of a regular geometric model fit to the surface of the earth. The faces of the geometric model provide an appropriate compromise between large-enough areas of coverage and small-enough distortion characteristics of the map projection upon them. The plane grid is placed in a triangular pattern with a regular geometry for varying the density, and with several options for addressing the points.

ACKNOWLEDGMENTS

We would like to acknowledge the contributions of Waldo Tobler, Geoffrey Dutton, Hrovoje Lukatela, and Michael Goodchild to our understanding of the issues in global geometry, and to thank John Snyder for inspiration and advice on map projections. We also thank Rick Linthurst, Jay Messer, and Dan McKenzie of EPA's Environmental Monitoring and Assessment Program for encouraging and sponsoring our work. This research has been supported by EPA contracts 68-C8-0006 with METI, 68-03-3439 with Kilkelly Environmental Associates, 68-C0-0021 with Technical Resources Inc., and cooperative agreement CR816721 with Oregon State University.

REFERENCES

Bailey, H.P. 1956. "Two Grid Systems that Divide the Entire Surface of the Earth into Quadrilaterals of Equal Area." *Transactions, American Geophysical Union*, vol. 37, no. 5, pp. 628-635.

Bradley, A.D. 1946. "Equal-Area Projection on the Icosahedron." *Geographical Review*, vol. 36, no. 1, pp. 101-104.

Christaller, W. 1966. *The Central Places of Southern Germany*, translated by C. Baskin. Englewood Cliffs, New Jersey: Prentice Hall.

Cochran, W.G. 1977. *Sampling Techniques*, third edition. New York: John Wiley and Sons.

Coxeter, H.S.M. 1948. *Regular Polytopes*. London: Methuen and Company Ltd.

Coxeter, H.S.M. 1969. *Introduction to Geometry*, second edition. New York: John Wiley and Sons.

Dacey, M.F. 1964. "A Note on Some Number Properties of a Hexagonal Hierarchical Plane Lattice." *Journal of Regional Science*, vol. 5, no. 2, pp. 63-67.

Dutton, G.H. 1989. "Modeling Locational Uncertainty via Hierarchical Tessellation." *Accuracy of Spatial Databases*, M.F. Goodchild and S. Gopal (eds.). London: Taylor & Francis.

Fekete, G. 1990. "Sphere Quadtrees: A New Data Structure to Support the Visualization of Spherically Distributed Data." *Proceedings of the SPIE/SPSE Symposium on Electronic Imaging Science and Technology*.

Gargantini, I. 1982. "An Effective Way to Represent Quadtrees." *Communications of the Association for Computing Machinery*, vol. 25, no. 12, pp. 905-910.

Gasson, P.C. 1983. *Geometry of Spatial Forms*. Chichester, England: Ellis Horwood Limited.

Gibson, L., and D. Lucas. 1982. "Spatial Data Processing Using Balanced Ternary." *Proceedings of the IEEE Computer Society Conference on Pattern Recognition and Image Processing*, pp. 566-571.

Goodchild, M.F., and Y. Shiren. 1989. "A Hierarchical Spatial Data Structure for Global Geographic Information Systems." Technical Paper 89-5, National Center for Geographic Information and Analysis, University of California, Santa Barbara.

Hudson, J.C. 1967. "An Algebraic Relation between the Lösch and Christaller Central Place Networks." *The Professional Geographer*, vol. 19, no. 3, pp. 133-135.

Lindgren, C.E.S. 1967. "The Geometry of Mixed Hexagonal Hierarchies in the Context of Central Place Theory." Harvard Papers in Theoretical Geography No. 7. Laboratory for Computer Graphics and Spatial Analysis, Graduate School of Design, Harvard University.

Lösch, A. 1954. *The Economics of Location*, translated by W.H. Woglom and W.F. Stolper. New Haven, Connecticut: Yale University Press.

Lukatela, H. 1987. "Hipparchus Geopositioning Model: An Overview." *Proceedings, Auto-Carto 8*, pp. 87-96.

Lyusternik, L.A. 1963. *Convex Figures and Polyhedra*, translated by T.J. Smith. New York: Dover Publications.

Mandelbrot, B.B. 1988. "Fractal Landscapes without Creases and with Rivers." *The Science of Fractal Images*, H.O. Peitgen and D. Saupe (eds.). New York: Springer-Verlag.

Matérn, B. 1986. *Spatial Variation*, second edition. Lecture Notes in Statistics, no. 36. Berlin: Springer-Verlag.

Mark, D.M., and J.P. Lauzon. 1985. "Approaches for Quadtree-Based Geographic Information Systems at Continental or Global Scales." *Proceedings, Auto-Carto 7*, pp. 355-364.

Messer, J.J., R.A. Linthurst, and W.S. Overton. 1991. "An EPA Program for Monitoring Ecological Status and Trends." *Environmental Monitoring and Assessment,* no. 17, pp. 67-78.

Morton, G. 1966. "A Computer-Oriented Geodetic Data Base, and a New Technique in File Sequencing." Internal memorandum, International Business Machines, Canada, Ltd.

Olea, R.A. 1984. "Sampling Design Optimization for Spatial Functions." *Mathematical Geology,* vol. 16, no. 4, pp. 369-392.

Paul, M.K. 1973. "On Computation of Equal Area Blocks." *Bulletin Geodésique,* no. 107, pp. 73-84.

Pearce, P., and S. Pearce. 1978. *Polyhedra Primer.* New York: Van Nostrand Reinhold Company.

Popko, E. 1968. *Geodesics.* Detroit: University of Detroit Press.

Richardson, L.F. 1961. "The Problem of Contiguity." *General Systems,* no. 6, pp. 139-187.

Samet, H. 1984. "The Quadtree and Related Hierarchical Data Structures." *Association for Computing Machinery Computing Surveys,* vol. 16, no. 2, pp. 187-260.

Snyder, J.P. 1987. *Map Projections—A Working Manual.* U.S. Geological Survey Professional Paper 1395.

Snyder, J.P. 1991. "An Equal-Area Map Projection for Polyhedral Globes." Manuscript submitted for publication.

Switzer, P. 1975. "Estimation of the Accuracy of Qualitative Maps." *Display and Analysis of Spatial Data,* J.C. Davis and M.J. McCullagh (eds.). New York: John Wiley and Sons.

Tobler, W., and Z-t. Chen. 1986. "A Quadtree for Global Information Storage." *Geographical Analysis,* vol. 18, no. 4, pp. 360-371.

Upton, G., and B. Fingleton. 1985. *Spatial Data Analysis by Example: Point Pattern and Quantitative Data.* Chichester, England: John Wiley and Sons.

U.S. Geological Survey. 1985 and other dates. "Indices to Topographic and Other Map Coverage" (by state). National Mapping Division.

van Roessel, J.W. 1988. "Conversion of Cartesian Coordinates from and to Generalized Balanced Ternary Addresses." *Photogrammetric Engineering and Remote Sensing,* vol. 54, no. 11, pp. 1565-1570.

Wickman, F.E., E. Elvers, and K. Edvarson. 1974. "A System of Domains for Global Sampling Problems." *Geografisker Annaler, Series A,* vol. 56, nos. 3-4, pp. 201-212.

Woldenberg, M.J. 1979. "A Periodic Table of Spatial Hierarchies." *Philosophy in Geography,* S. Gale and G. Olsson (eds.). Dordrecht, The Netherlands: D. Reidel Publishing Company.